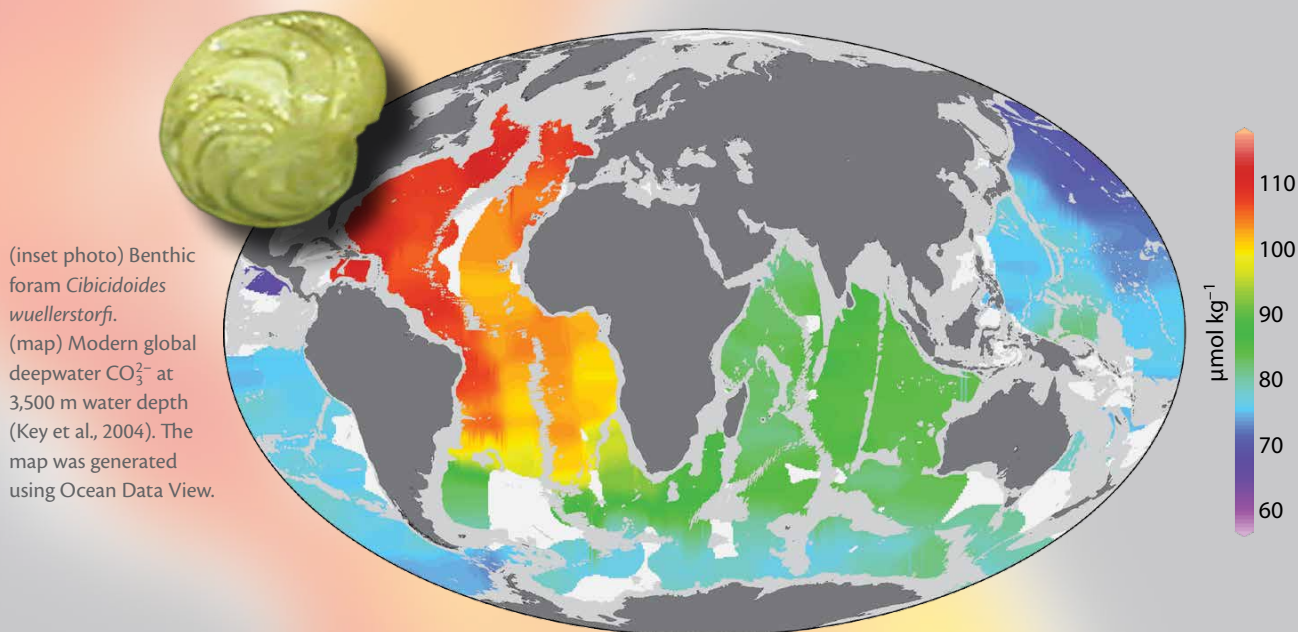# Deep Ocean Carbonate Chemistry and Glacial-Interglacial Atmospheric CO$_2$ Changes

BY JIMIN YU, ROBERT F. ANDERSON, AND EELCO J. ROHLING

(inset photo) Benthic foram *Cibicidoides wuellerstorfi*.
(map) Modern global deepwater CO$_3^{2-}$ at 3,500 m water depth (Key et al., 2004). The map was generated using Ocean Data View.

ABSTRACT. Changes in deep ocean carbonate chemistry have profound implications for glacial-interglacial atmospheric CO$_2$ changes. Here, we review deep ocean carbonate ion concentration ([CO$_3^{2-}$]) changes based on the benthic foraminiferal boron-to-calcium ratio (B/Ca) and their links to global carbon reorganization since the last ice age. Existing deep ocean [CO$_3^{2-}$] reconstructions are consistent with changes in the biological pump, in ocean stratification, and in the associated oceanic alkalinity inventory as key mechanisms for modulating atmospheric CO$_2$ on glacial-interglacial time scales. We find that the global mean deep ocean [CO$_3^{2-}$] was roughly similar between the Last Glacial Maximum (LGM; 18,000–22,000 years ago) and the Late Holocene (0–5,000 years ago). In view of elevated glacial surface [CO$_3^{2-}$], this indicates enhanced storage of respiratory carbon in a more alkaline deep ocean during the LGM. During early deglaciation, rising [CO$_3^{2-}$] at three locations in the deep ocean suggests a release of deep-sea CO$_2$ to the atmosphere, probably via the Southern Ocean. Both increased late deglacial carbonate burial in deep-sea sediments due to elevated [CO$_3^{2-}$] and Holocene expansion of coral reefs on newly flooded continental shelves depleted global ocean alkalinity, which reduced CO$_2$ solubility in seawater and contributed to atmospheric CO$_2$ rises at these times.

INTRODUCTION

One of the most intriguing findings in paleoclimate research concerns systematic glacial-interglacial atmospheric CO_2 variations, as revealed by measurements of air bubbles trapped in ice cores from Antarctica. During the last 800,000 years, atmospheric CO_2 fluctuations have been highly correlated with climate on millennial time scales (Figure 1; Lisiecki and Raymo, 2005; Jouzel et al., 2007; Lüthi et al., 2008). Because CO_2 is a greenhouse gas, atmospheric CO_2 fluctuations likely caused, or at least amplified, the climatic changes. Thus, resolving the reasons for glacial-interglacial atmospheric CO_2 fluctuations is essential for improved understanding of the mechanisms that control the global climate system.

Despite intensive research, the mechanisms for past atmospheric CO_2 changes remain elusive. Because the ocean is the largest carbon reservoir that equilibrates with the atmosphere on a ~ 1,000 year time scale, Broecker (1982) argued that the ocean must have played a critical role in modulating past atmospheric CO_2 variations. Changes in physical conditions, including temperature, salinity, and ocean volume (due to waxing and waning of ice sheets; Figure 1), have opposing effects, resulting in a net decrease in atmospheric CO_2 by ~ 15 ppm during glacials (Sigman and Boyle, 2000; Brovkin et al., 2007). This decrease is barely enough to counter the atmospheric CO_2 rise that is due to the transport of ~ 500 Gt (1 Gt = 10^{15} g) of carbon from the land biosphere to the ocean during interglacial to glacial transitions (Bird et al., 1994; Ciais et al., 2012). To explain up to ~ 100 ppm glacial-interglacial atmospheric CO_2 fluctuations requires more complex ocean processes. Existing evidence suggests that biogeochemistry and physical

circulation changes, especially in the Southern Ocean, are critical (Sigman and Boyle, 2000; Stephens and Keeling, 2000; Toggweiler et al., 2006; Anderson et al., 2009; Sigman et al., 2010).

Deepwater carbonate ion concentration, $[CO_3^{2-}]$, is a critical parameter in investigations of carbon reorganization in the climate system. To a first approximation, $[CO_3^{2-}] \approx ALK - DIC$ (Zeebe and Wolf-Gladrow, 2001), where ALK is alkalinity and DIC is dissolved inorganic carbon (DIC = $[CO_2] + [HCO_3^-] + [CO_3^{2-}]$), both of which affect atmospheric CO_2 (Figure 2). ALK represents the excess base that affects deprotonation of aqueous CO_2 into bicarbonate ion (HCO_3^-) and CO_3^{2-}. Everything else being equal, an increase in ALK causes more DIC to take the form of CO_3^{2-} and less of it to be aqueous CO_2, lowering CO_2 partial pressure (Figure 2B) and effectively increasing CO_2 solubility in seawater and decreasing atmospheric CO_2. Deepwater $[CO_3^{2-}]$ determines seawater carbonate saturation, affecting dissolution/

preservation of $CaCO_3$ on the seafloor and, hence, the global oceanic ALK inventory. Reconstruction of deep ocean $[CO_3^{2-}]$ chemistry changes therefore can elucidate critical processes and mechanisms in the past global carbon cycle. We review recent progress in such reconstructions since the last ice age, along with the impacts on atmospheric CO_2 changes.

MODERN OCEAN $[CO_3^{2-}]$ VARIABILITY

We first summarize variations in $[CO_3^{2-}]$ and factors controlling them in the modern ocean (Figure 3; Key et al., 2004). In general, surface-ocean $[CO_3^{2-}]$ is elevated relative to the deep ocean. Temperature and salinity changes have small effects on seawater $[CO_3^{2-}]$, with sensitivities of 0.5 µmol kg^{-1} per °C and –0.5 µmol kg^{-1} per ‰, respectively (Yu et al., 2008). The elevated surface $[CO_3^{2-}]$ is predominantly caused by conversion of DIC and ALK into biological particles during phytoplankton photosynthesis in the euphotic zone (less than ~ 150 m). At a rain ratio
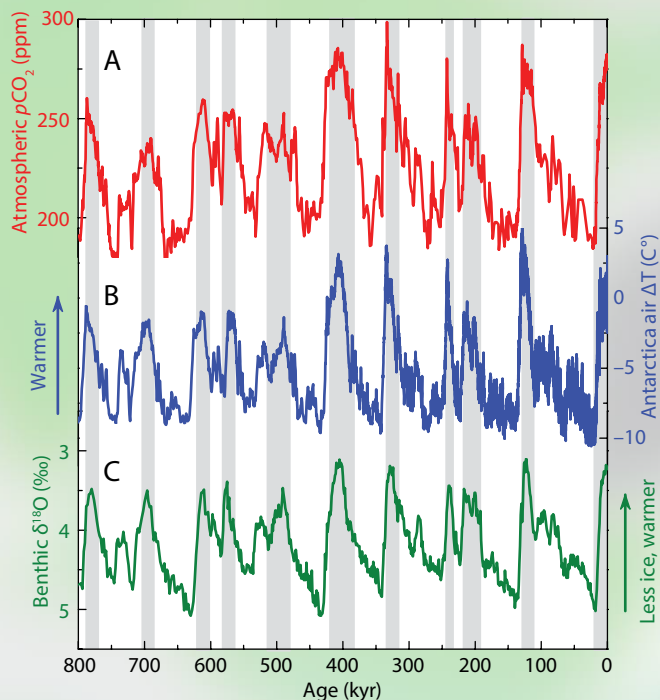

Figure 1. Records of (A) atmospheric pCO_2 (Lüthi et al., 2008) compared with (B) Antarctic air temperature changes (Jouzel et al., 2007) and (C) benthic foraminiferal $\delta^{18}O$ stack curve (Lisiecki and Raymo, 2005) during the last 800,000 years. Vertical gray bars indicate interglacials.

($C_{organic}$:C_{CaCO_3}) of 4:1 (Broecker and Peng, 1982), photosynthesis consumes seawater DIC and ALK at a ratio of 3.58:1 (Yu et al., 2008) and leads to an increase in seawater [CO_3^{2-}] (Figure 2A). Different from other regions, the Southern Ocean exhibits reduced surface-deep water [CO_3^{2-}] contrast (Figure 3A), due to intensive upwelling of very deep waters and inefficient nutrient utilization (Broecker et al., 1998).

Sinking and subsequent decomposition of biological matter decreases [CO_3^{2-}] in the deep ocean (Figure 2A), but different water masses bear distinctive values that reflect their different histories (Figure 3). The well-ventilated North Atlantic Deep Water (NADW) has the highest [CO_3^{2-}], ~ 120 μmol kg^{-1}, and the poorly ventilated North Pacific Deep Water (NPDW) has the lowest [CO_3^{2-}], ~ 50 μmol kg^{-1}. Lower

Circumpolar Deep Water (LCDW) and Antarctic Intermediate Water (AAIW), both formed in the Southern Ocean, have intermediate [CO_3^{2-}] values of ~ 80 μmol kg^{-1}. The [CO_3^{2-}] gradient along the deepwater pathway from the North Atlantic to the North Pacific reflects gradual accumulation of remineralized biological matter, which is also indicated by higher DIC in the deep equatorial Pacific, by ~170 μmol kg^{-1}, than in the deep equatorial Atlantic Ocean (Figure 3C). Ocean circulation imposes secondary features on the general decrease in [CO_3^{2-}] with increasing water depth. For example, northward penetration of AAIW produces a [CO_3^{2-}] minimum at ~ 850 m in the equatorial Atlantic Ocean, while southward advection of low-[CO_3^{2-}] NPDW leads to a [CO_3^{2-}] minimum at ~ 700 m in the equatorial Pacific Ocean (Figure 3B).

Although less obvious, deep water [CO_3^{2-}] is also significantly affected by ALK changes associated with $CaCO_3$ dissolution on the seafloor, especially in the Pacific Ocean. In the equatorial Pacific Ocean, waters below ~ 2.5 km are mainly sourced from the Southern Ocean. Compared to waters at ~ 5 km water depth, the southward return flow at ~ 3 km has stayed in the deep ocean for a longer time and, hence, has accumulated more remineralized DIC and ALK (Schmitz, 1996). As a consequence, DIC is ~ 50 μmol kg^{-1} higher at 3 km water depth than at 5 km water depth in the equatorial Pacific (Figure 3C). Were this DIC increase solely due to remineralization of biological particles sinking from the surface, then ALK would be expected to rise by ~ 15 μmol kg^{-1}, which is less than the observed increase of ~ 40 μmol kg^{-1}. This discrepancy suggests an introduction of ALK into deep waters by $CaCO_3$ dissolution on the seafloor. Compared to the deep equatorial Atlantic Ocean, the observed ~ 25 μmol kg^{-1} decrease in deep equatorial Pacific [CO_3^{2-}] corresponds to shoaling of the calcite saturation horizon by ~ 1.3 km (Figure 3B), deterioration of the calcite saturation degree, and promotion of $CaCO_3$ dissolution in the Pacific Ocean. As a consequence, the calcite lysocline—the depth where $CaCO_3$ dissolution intensifies
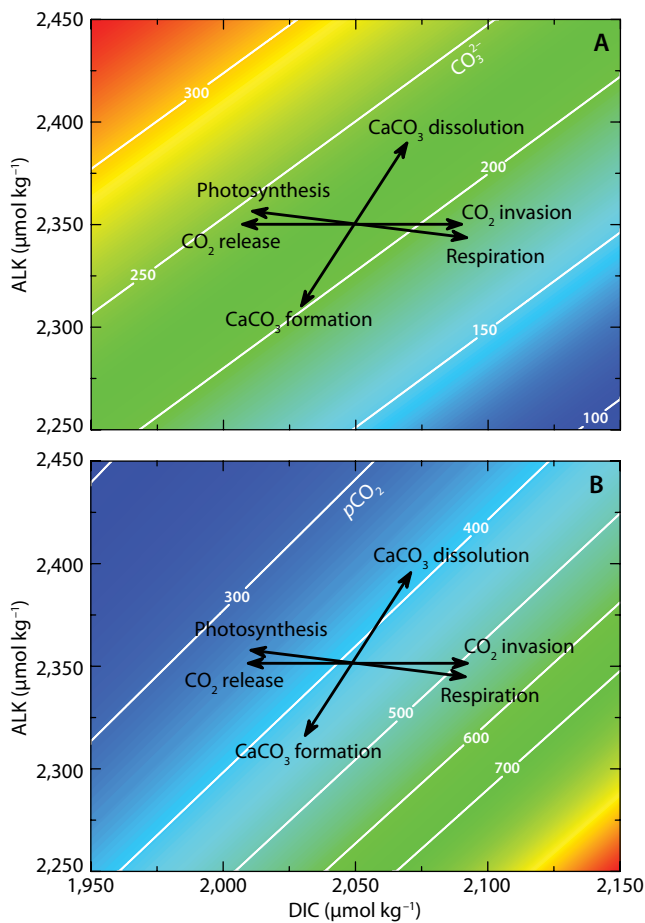

Figure 2. Effects of various processes on (A) carbonate ion concentration, [CO_3^{2-}], and (B) pCO_2 in ALK–DIC space (ALK = alkalinity and DIC = dissolved inorganic carbon). Seawater [CO_3^{2-}] (unit: μmol kg^{-1}) and pCO_2 (unit: μatm) are calculated at temperature of 25°C, salinity of 35, pressure of 1 atm (water depth of 0 m). $CaCO_3$ dissolution increases seawater ALK and DIC in a ratio of 2:1, with a net effect to raise seawater [CO_3^{2-}] and decrease pCO_2; $CaCO_3$ formation has the opposite effects. Invasion and release of CO_2 into/from the ocean only affects seawater DIC. Photosynthesis mainly consumes seawater DIC and slightly increases seawater ALK due to the uptake of nitrate; respiration has the reverse effect.

Jimin Yu (*jimin.yu@anu.edu.au*) *is Fellow, Research School of Earth Sciences, The Australian National University, Canberra, Australia.* **Robert F. Anderson** *is Ewing Lamont Research Professor, Lamont-Doherty Earth Observatory of Columbia University, Palisades, NY, USA.* **Eelco J. Rohling** *is Professor, Research School of Earth Sciences, The Australian National University, Canberra, Australia.*

in sediments, which is highly coupled with the calcite saturation horizon in the modern ocean (Broecker and Takahashi, 1978)—is ~ 1 km shallower in the Pacific Ocean than in the Atlantic Ocean. $CaCO_3$ dissolution adds ALK and DIC to seawater at a ratio of 2:1 and increases seawater $[CO_3^{2-}]$ (Figure 2A). In a sense, $CaCO_3$ dissolution in the deep Pacific Ocean serves as a buffering mechanism to reduce decreases in $[CO_3^{2-}]$ and pH caused by the remineralization of sinking biological matter.

BENTHIC B/CA AS A PROXY FOR DEEPWATER $[CO_3^{2-}]$

Because of its sensitivity to deepwater saturation degree, $CaCO_3$ preservation in sediments has been used to estimate deepwater $[CO_3^{2-}]$ (e.g., Crowley, 1983; Farrell and Prell, 1989; Le and Shackleton, 1992; Anderson and Archer, 2002). However, estimates of $CaCO_3$ dissolution-based proxies are mostly qualitative and are complicated by factors such as dissolution in pore waters and surface water condition changes (Archer and Maier-Reimer, 1994; Barker and Elderfield, 2002), and they become insensitive at shallow water depths where seawater is generally supersaturated and carbonate dissolution is minimal. Recent core-top studies show that boron isotope ratios ($\delta^{11}B$) in some benthic foraminiferal species are useful for reconstructing deepwater pH and $[CO_3^{2-}]$, but down-core $\delta^{11}B$ measurements are of low temporal resolution and limited to a few locations, partially due to the relatively large sample size requirement for analyses (Hönisch et al., 2008; Yu et al., 2010b; Rae et al., 2011). Some empirical approaches have also been developed to quantify deepwater $[CO_3^{2-}]$. For example, the partitioning of Zn into benthic foraminiferal

carbonates appears to be correlated with the degree of deepwater calcite saturation ($\Delta[CO_3^{2-}]$, defined by $\Delta[CO_3^{2-}] = [CO_3^{2-}]_{in\ situ} - [CO_3^{2-}]_{sat}$, where $[CO_3^{2-}]_{sat}$ is $[CO_3^{2-}]$ for $CaCO_3$ saturation at in situ temperature and pressure) at $\Delta[CO_3^{2-}]$ values below ~ 25 μmol kg^{-1}. However, the prerequisite to knowing past seawater [Zn], which is nontrivial, makes application of this method a challenge (Marchitto et al., 2000).

Here, we focus on a recently developed empirical proxy, which uses the benthic foraminiferal boron-to-calcium ratio (B/Ca). The method is supported by extensive core-top calibrations (Figure 4; Yu and Elderfield, 2007; Brown et al., 2011; Rae et al., 2011; Raitzsch et al., 2011; Yu et al., 2013a) and has been applied to all three major ocean basins across the last glacial-interglacial transition (Figure 5; Yu et al., 2008, 2010a,
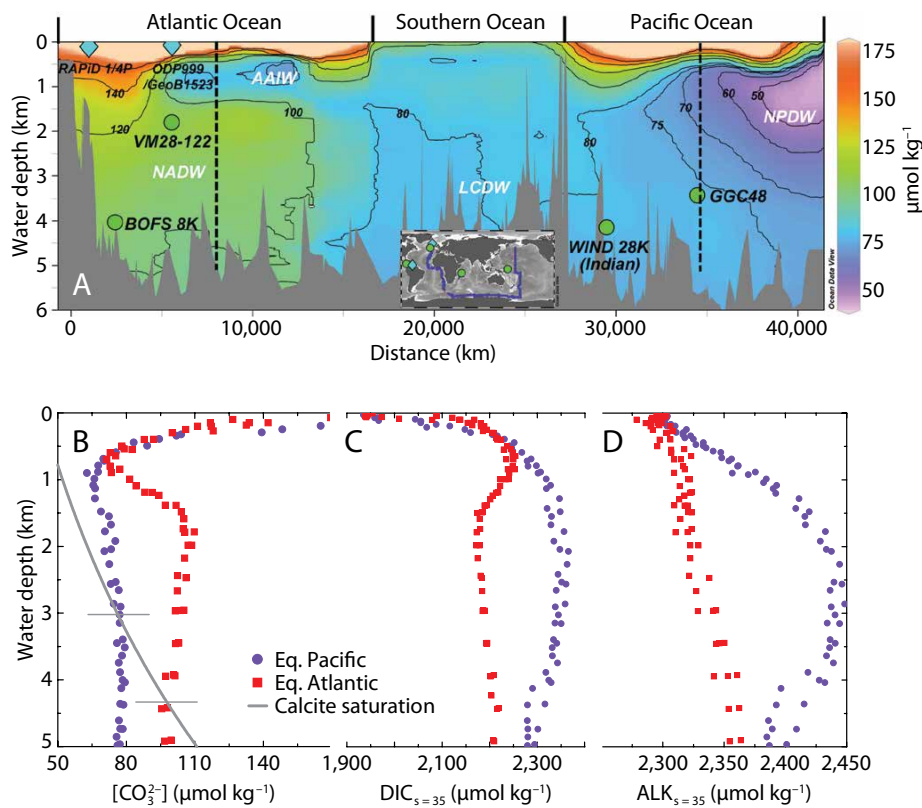

Figure 3. (A) Distribution of seawater $[CO_3^{2-}]$ in the global modern ocean. Four water masses are indicated: NADW = North Atlantic Deep Water, AAIW = Antarctic Intermediate Water, LCDW = Lower Circumpolar Deep Water, and NPDW = North Pacific Deep Water. Inset shows the locations of hydrographic sites used for the $[CO_3^{2-}]$ section. Circles and diamonds show, respectively, the locations of cores for deep and surface water $[CO_3^{2-}]$ reconstructions displayed in Figure 6. Vertical dashed lines indicate locations of hydrographic sites for depth profiles shown in (B–D). (B) Bathymetric profile of $[CO_3^{2-}]$ with salinity normalized to account for effects of mixing and evaporation-precipitation. (C) and (D) Bathymetric profiles, respectively, of DIC and ALK in the equatorial Atlantic and Pacific Oceans. (B) also shows calcite saturation $[CO_3^{2-}]$ and the saturation horizons in equatorial Atlantic and Pacific Oceans. The saturation horizon is defined as the depth where in situ $[CO_3^{2-}]$ equals the saturation $[CO_3^{2-}]$ (which is largely determined by pressure or water depth). Above the saturation horizon, seawater is saturated and $CaCO_3$ tends to be preserved, whereas below the saturation horizon, seawater is undersaturated and $CaCO_3$ has the potential to dissolve. Panel (A) is generated using Ocean Data View (Schlitzer, 2006). Data are from the GLobal Ocean Data Analysis Project (GLODAP) data set (Key et al., 2004).

2013a; Rickaby et al., 2010; Raitzsch et al., 2011). As Figure 4 shows, B/Ca in the species *Cibicidoides wuellerstorfi* and *Cibicidoides mundulus* shows clear linear relationships with deepwater $\Delta[CO_3^{2-}]$, and there appears to be no threshold in the B/Ca:$\Delta[CO_3^{2-}]$ sensitivity at high $\Delta[CO_3^{2-}]$, allowing reconstructions using shallow sites. Both *C. wuellerstorfi* and *C. mundulus* are epifaunal species, with a habitat above the sediment-seawater interface (Lutze and Thiel, 1989), which minimizes complications in B/Ca due to pore water chemistry. Because B is conservative in seawater, changes in the B concentration or inventory over time scales of 14–20 million years (Lemarchand et al., 2000) have limited influence. Existing data suggest an absence of temperature and dissolution effects on benthic B/Ca (Yu and Elderfield, 2007). In addition, the method requires small sample sizes, which facilitates its use to generate

detailed records. Seawater $[CO_3^{2-}]_{sat}$ is largely determined by water depth (pressure) and remains roughly unchanged in the deep ocean on glacial-interglacial time scales. Thus, the correlations shown in Figure 4 provide an empirical approach to reconstructing past deepwater $[CO_3^{2-}]$ using benthic B/Ca by $[CO_3^{2-}] = \Delta[CO_3^{2-}] + [CO_3^{2-}]_{sat}$.

The underlying mechanisms that control the benthic B/Ca proxy require future study. The B/Ca–$\Delta[CO_3^{2-}]$ correlations may be partly linked to B speciation in seawater. B exists as boric acid ($B(OH)_3$) and borate ($B(OH)_4^-$) in seawater, but only the charged species $B(OH)_4^-$ is thought to be incorporated into marine carbonates (Hemming and Hanson, 1992). As pH increases, seawater CO_3^{2-} and $B(OH)_4^-$ concentrations generally (but not linearly) increase (Zeebe and Wolf-Gladrow, 2001), which would increase B/Ca in benthic foraminiferal carbonates and

lead to a positive correlation between CO_3^{2-} and B/Ca. However, the relationships considered here concern benthic B/Ca against $\Delta[CO_3^{2-}]$ (Figure 4), which includes both in situ $[CO_3^{2-}]$ and $[CO_3^{2-}]_{sat}$ (a pressure effect). In addition, the foraminiferal calcification rate, which is partially affected by seawater $\Delta[CO_3^{2-}]$, may impose some influence on B/Ca. Different B/Ca ranges and B/Ca:$\Delta[CO_3^{2-}]$ sensitivities between *C. wuellerstorfi* and *C. mundulus* also suggest biological influences on B incorporation into benthic foraminiferal carbonate. Despite incomplete understanding of the mechanisms, a down-core comparison between benthic B/Ca and $\delta^{11}B$ (Yu et al., 2010b) strongly supports the feasibility of the core-top calibrations for past deepwater $[CO_3^{2-}]$ reconstructions as shown in Figure 4. Currently, calibrations are only available for a few species, and B/Ca in other benthic species remains to be explored.
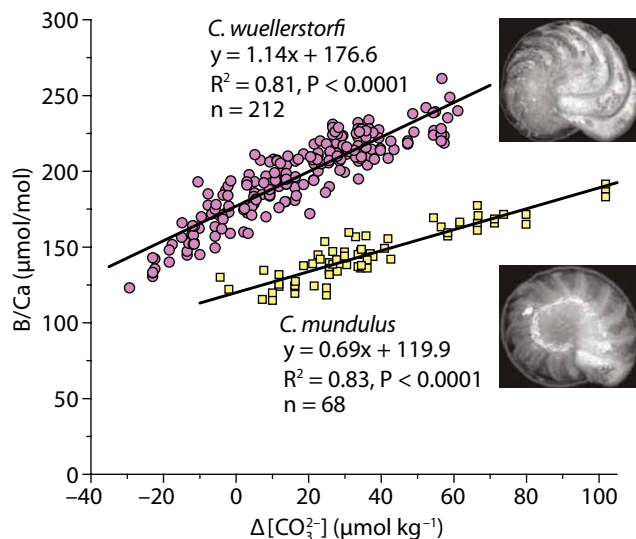

Figure 4. Benthic foraminiferal B/Ca proxy for deepwater $[CO_3^{2-}]$ (Yu and Elderfield, 2007; Brown et al., 2011; Rae et al., 2011; Raitzsch et al., 2011; Yu et al., 2013a). In seawater, $\Delta[CO_3^{2-}] = [CO_3^{2-}]_{in\ situ} - [CO_3^{2-}]_{sat}$, where $[CO_3^{2-}]_{sat}$ represents saturation $[CO_3^{2-}]$ and remains roughly stable on glacial-interglacial time scales. Benthic B/Ca can be converted into $\Delta[CO_3^{2-}]$ using the calibrations shown in this figure. Deepwater $[CO_3^{2-}]$ is then calculated by $[CO_3^{2-}] = \Delta[CO_3^{2-}] + [CO_3^{2-}]_{sat}$. The images show morphologies of umbilical sides of the two species (Rae et al., 2011). See http://www.foraminifera.eu for more species images.
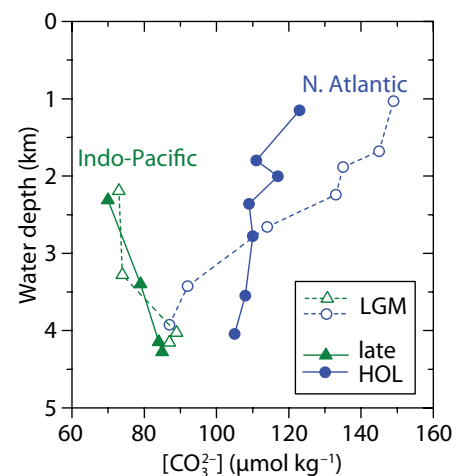

Figure 5. Bathymetric distribution of seawater $[CO_3^{2-}]$ in the North Atlantic and Indo-Pacific Oceans during the Late Holocene (0-5,000 years ago) and the Last Glacial Maximum (LGM; 18,000–22,000 years ago) (Yu et al., 2013a).

DOWN-CORE [CO$_3^{2-}$] RECONSTRUCTIONS AND IMPLICATIONS FOR PAST ATMOSPHERIC CO$_2$ CHANGES

Last Glacial Maximum

Figure 5 shows bathymetric distributions of benthic B/Ca-derived deepwater [CO$_3^{2-}$] in the North Atlantic and Indo-Pacific Oceans during the Last Glacial Maximum (LGM; 18,000–22,000 years ago) and Late Holocene (0–5,000 years ago) (Yu et al., 2013a). The large LGM-to-Holocene [CO$_3^{2-}$] changes from about +20 to –35 µmol kg^{-1} in the North Atlantic Ocean are consistent with substantial changes in the geometry of Atlantic Meridional Ocean Circulation. During the LGM, Glacial North Atlantic Intermediate Water (GNAIW) was characterized by low nutrient content, high δ^{13}C, and high [CO$_3^{2-}$] values, and sank to ~ 2.5 km in the North Atlantic (Boyle and Keigwin, 1987; Curry and Oppo, 2005; Yu et al., 2008). Below GNAIW were Antarctic-derived waters with high-nutrient, low-δ^{13}C, and low-[CO$_3^{2-}$] properties (Figures 3A and 5). During the LGM, elevated [CO$_3^{2-}$] at the mid-depth range likely resulted from high surface preformed [CO$_3^{2-}$] in the North Atlantic (Figure 6A,B) (Henehan et al., 2013; Yu et al., 2013b), while decreased [CO$_3^{2-}$] in the deep North Atlantic is consistent with a greater penetration of low-[CO$_3^{2-}$] deep waters from the Southern Ocean (Figure 3A; Curry and Oppo, 2005).

Because (1) the Atlantic is relatively small in volume (~ 25% of the global ocean), and (2) opposite changes in [CO$_3^{2-}$] at shallow and deep water masses tend to cancel each other, changes in Atlantic [CO$_3^{2-}$] have negligible impacts on the global mean deep ocean [CO$_3^{2-}$]. In contrast, LGM-to-Holocene [CO$_3^{2-}$] changes in the deep Indo-Pacific Oceans (accounting for ~75% of the global

deep-sea volume) are within about ±5 µmol kg^{-1}, implying efficient buffering of deepwater pH by deep-sea CaCO$_3$ dissolution in these basins (Anderson and Archer, 2002). Our reconstructions are different from the large [CO$_3^{2-}$] changes inferred in an the early study using δ^{11}B (Sanyal et al., 1995), which were likely compromised due to the use of mixed benthic foraminiferal species.

Supported by foraminiferal assemblage estimates and a modest change in calcite lysocline depth in the Pacific Ocean (Catubig et al., 1998; Anderson and Archer, 2002), the small LGM-to-Holocene [CO$_3^{2-}$] contrast in the deep Indian and Pacific Oceans (Yu et al., 2013a) suggests comparable global mean deep ocean [CO$_3^{2-}$] between the LGM and the Late Holocene. This places
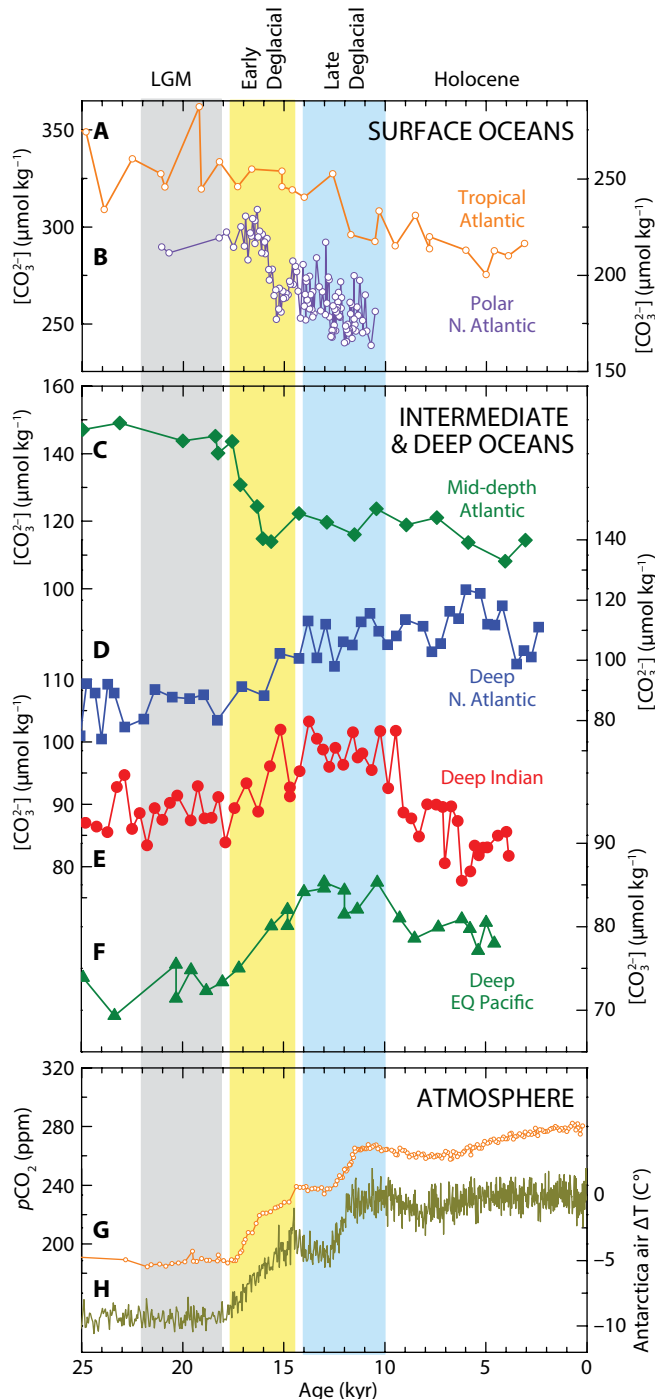

Figure 6. Surface (top panel) and deep (middle panel) ocean [CO$_3^{2-}$] compared with atmospheric records (bottom panel) during the last 25,000 years. Surface water [CO$_3^{2-}$] records are for composite results from cores from (A) ODP 999 (13°N, 79°W) and GeoB1523-1 (4°N, 42°W) (Henehan et al., 2013) and from (B) RAPiD 1P (62.3°N, 17.6°W) and 4P (62.3°N, 17.1°W) (Yu et al., 2013b). Deepwater [CO$_3^{2-}$] data are from samples from cores (C) VM28-122 (12°N, 79°W, 3,623 m; sill depth = 1,800 m) (Yu et al., 2010b), (D) BOFS 8K (52.5°N, 22.1°W, 4,045 m) (Yu et al., 2008), (E) WIND 28K (10.2°S, 51.8°E, 4,147 m) (Yu et al., 2010a), and (F) GGC48 (0°, 161°E, 3,400 m) (Yu et al., 2010a). Core locations are shown in Figure 3A. Atmospheric pCO$_2$ (G) and Antarctic air temperature change (H) are based on ice core reconstructions (Jouzel et al., 2007; Lüthi et al., 2008).

important constraints on factors influencing the global carbon cycle and low atmospheric CO_2 during glacials.

During the LGM, atmospheric CO_2 was ~ 90 ppm lower than during the pre-industrial period (Figure 6G; Lüthi et al., 2008). Assuming equilibrium between the surface ocean and the atmosphere, surface water $[CO_3^{2-}]$ during the LGM

with reduced dissolved O_2 concentrations in the glacial deep Pacific Ocean (Galbraith et al., 2007; Bradtmiller et al., 2010; Jaccard and Galbraith, 2012). It also agrees with inferences of increased biological pump efficiency and enhanced stratification in the glacial ocean (Kumar et al., 1995; Lund et al., 2011; Burke and Robinson, 2012), which would have

allowed more corrosive Southern-sourced deep waters (Figure 3A) to occupy the deep Atlantic, further strengthening $CaCO_3$ dissolution there (Figure 6D). Moreover, reduced coral growth during glacial times due to substantial shrinkage of shelf areas caused by ~ 120 m sea level drop (e.g., Grant et al., 2012) reduced the removal of ALK by reef aragonite on continental shelves (Opdyke and Walker, 1992). Assuming stable ALK input from rivers and unchanged pelagic $CaCO_3$ production, reduced $CaCO_3$ accumulation in deep-sea sediments and on shelves would upset the oceanic ALK balance between riverine input and marine burial. This activates carbonate compensation, a negative feedback to bring the ocean carbonate system back to a new steady state (Broecker and Peng, 1987). Reduced $CaCO_3$ burial introduces ALK and DIC in a 2:1 ratio into the ocean, causing oceanic $[CO_3^{2-}]$ to rise (Figure 2A) until the ALK balance is restored on a time scale of ~ 5,000 years (Broecker and Peng, 1987). A net ALK gain occurred during glaciations. By increasing CO_2 solubility in seawater, increased ocean ALK helps to further lower atmospheric CO_2 during glaciations (Figure 2B; Broecker and Peng, 1987; Boyle, 1988).

> ## CHANGES IN DEEP OCEAN CARBONATE CHEMISTRY HAVE PROFOUND IMPLICATIONS FOR GLACIAL-INTERGLACIAL ATMOSPHERIC CO_2 CHANGES.

would have been ~ 60 μmol kg^{-1} higher than at pre-industrial times (a rule of thumb: seawater pCO_2 and $[CO_3^{2-}]$ are inversely correlated; Figure 2), which is supported by surface water reconstructions in the tropical and polar North Atlantic Ocean (Figure 6A,B; Henehan et al., 2013; Yu et al., 2013b). Although not yet fully established, it is therefore reasonable to expect that the surface source waters for newly formed deep waters had a substantially higher pre-formed $[CO_3^{2-}]$ during the LGM than today (pre-industrial). Similarity of deepwater $[CO_3^{2-}]$ values between the LGM and the Late Holocene then suggests an enhanced surface-to-deep $[CO_3^{2-}]$ gradient in the LGM ocean. This requires a larger amount of respiratory CO_2 stored in the deep sea during the LGM due to remineralization of biogenic matter, which titrated the higher pre-formed $[CO_3^{2-}]$ surface waters to deep-water $[CO_3^{2-}]$ values that were similar to those observed in the modern deep sea (Figure 2A). Increased respiratory CO_2 in the glacial deep sea is consistent

facilitated a buildup of CO_2 in the deep ocean and contributed to reduced glacial atmospheric CO_2 levels (Sigman and Boyle, 2000; Sigman et al., 2010).

During the LGM, the carbon lost from the atmosphere (~ 200 GtC) and the terrestrial biosphere (~ 500 GtC) must have been stored as DIC in the deep ocean (Broecker, 1982), assuming there were no significant changes in the ocean-atmosphere carbon inventory. Given the observed minor change in global mean deep ocean $[CO_3^{2-}]$ (Figure 5), deep ocean ALK ($\approx [CO_3^{2-}]$ + DIC) must have been substantially higher during the LGM than today. Elevated glacial oceanic ALK likely resulted from decreased $CaCO_3$ burial. Sequestration of excess respiratory CO_2 into the deep ocean during the transition from the last interglacial to the last ice age as a result of iron fertilization would have lowered deepwater $[CO_3^{2-}]$ (Figure 2A) and resulted in shoaling of the saturation horizon, which increased $CaCO_3$ dissolution on the seafloor. In addition, the replacement of NADW with GNAIW

The Last Deglaciation

Figure 6 shows benthic B/Ca-derived deepwater $[CO_3^{2-}]$ at four locations from the global deep ocean (middle panel), together with some surface water $[CO_3^{2-}]$ (top panel) and atmospheric CO_2 and Antarctic temperature changes (bottom panel) during the last 25,000 years. During the early deglaciation (17,500–14,500 years ago), $[CO_3^{2-}]$ rose by about 10 μmol kg^{-1} in the deep Atlantic, Indian, and equatorial Pacific Oceans (Figure 6D–F). This cannot

be explained by changes in preformed $[CO_3^{2-}]$ because surface $[CO_3^{2-}]$ declined during this time interval (Figure 6A,B). Because increasing deepwater $[CO_3^{2-}]$ would promote deep-sea $CaCO_3$ preservation and thus deplete the oceanic ALK inventory, a $[CO_3^{2-}]$ rise likely reflects a decrease in DIC (Yu et al., 2010a). Therefore, these deepwater $[CO_3^{2-}]$ increases during the early deglaciation are consistent with transfer of CO_2 from deep ocean basins into intermediate water depths (as indicated by a $[CO_3^{2-}]$ decline at mid-depth in the North Atlantic [Figure 6C]) and into the atmosphere (Figure 6G). Release of deep-sea CO_2 may have occurred by increased "leakage" of CO_2 in the Southern Ocean due to (1) reduced nutrient consumption caused by a decline in dust deposition in the Subantarctic Zone (Broecker and Henderson, 1998; Martinez-Garcia et al., 2011), (2) breakdown of ocean stratification in the Southern Ocean as suggested by opal flux and radiocarbon results (Anderson et al., 2009; Burke and Robinson, 2012), and (3) melting of sea ice, a physical barrier to sequestration of CO_2 in the ocean, induced by rapid warming around Antarctica (Figure 6H; Stephens and Keeling, 2000; Jouzel et al., 2007). The release of deep-sea CO_2 is suspected to be responsible for a ~ 50 ppm rise in atmospheric CO_2 and a ~ 190‰ decline in atmospheric radiocarbon during the early deglaciation (Broecker and Barker, 2007; Lüthi et al., 2008).

During the late deglaciation (14,000–10,000 years ago), the global deep ocean had elevated $[CO_3^{2-}]$ relative to the LGM, and Indo-Pacific records show plateaus in deepwater $[CO_3^{2-}]$ (Figure 6C,D). The little $[CO_3^{2-}]$ change in the deep Indo-Pacific at this time is counterintuitive, given continued

transfer of carbon amounting to ~ 450 GtC from the deep sea to the atmosphere and terrestrial biosphere as deduced from benthic $\delta^{13}C$ and atmospheric CO_2 (Lüthi et al., 2008; Yu et al., 2010a), which ought to drive up deepwater $[CO_3^{2-}]$ by decreasing DIC in deep ocean basins (Figure 2A). The absence of a rise in deep Indo-Pacific $[CO_3^{2-}]$ likely indicates an ALK decrease possibly associated with carbonate compensation (Broecker and Peng, 1987). The initial deepwater $[CO_3^{2-}]$ increase due to CO_2 release during the early deglaciation would promote the preservation and burial of $CaCO_3$ in sediments, which is observed at many locations worldwide from 14,000–10,000 years ago (Berger, 1977; Farrell and Prell, 1989, 1991; Hodell et al., 2001; Anderson et al., 2008; Yu et al., 2010a). Improved $CaCO_3$ preservation during the last deglaciation in turn decreased the oceanic ALK inventory and, hence, lowered oceanic $[CO_3^{2-}]$ (Figure 2A). Thus, the late deglacial $[CO_3^{2-}]$ plateau in the Indo-Pacific suggests a strong carbonate compensation effect that counteracted the rise in deepwater $[CO_3^{2-}]$ driven by CO_2 degassing. By reducing whole ocean alkalinity, carbonate compensation helps to release additional CO_2 from the deep ocean during deglaciations (Figure 2B).

The Holocene

Deepwater $[CO_3^{2-}]$ in the deep Indian and Pacific Oceans declined by 5–15 μmol kg^{-1} during the Holocene (0–10,000 years ago; Figure 6E,F). Ocean circulation changes may account for different magnitudes in this $[CO_3^{2-}]$ decline, as well as for the opposite $[CO_3^{2-}]$ changes observed in the Atlantic Ocean (Figure 6C,D). Because benthic $\delta^{13}C$ (which is sensitive to biological respiration) has remained roughly constant

(e.g., Yu et al., 2010a), the Holocene $[CO_3^{2-}]$ decline in the deep Indo-Pacific Oceans likely resulted from a depletion in oceanic ALK. This inferred ALK decrease is consistent with continued carbonate compensation in response to the carbon reorganization that occurred during the last deglaciation. Additionally, coral reef buildup on shelves due to an increase in the area of shallow water environments at high sea level stand may have contributed to the removal of ALK and resulted in a decrease in whole ocean $[CO_3^{2-}]$ (Opdyke and Walker, 1992). By reducing CO_2 solubility in the ocean, the decrease in the whole ocean ALK inventory drives up atmospheric CO_2 (Figure 2B) and contributes to the 20 ppm rise in atmospheric CO_2 since ~ 8,000 years ago (Figure 6G), as demonstrated by modeling (Ridgwell et al., 2003; Menviel and Joos, 2012).

SUMMARY

Deep-ocean $[CO_3^{2-}]$ is tightly linked to processes that affect carbon reorganization in the ocean and thus serves as a valuable tracer for investigations of the global carbon cycle. Reconstructions based on benthic foraminiferal B/Ca are consistent with a stronger biological pump, increased ocean stratification, and elevated global ocean alkalinity during the LGM, all of which contributed to reduced atmospheric CO_2 levels during ice ages. The synchronicity of an important early deglacial deep-sea $[CO_3^{2-}]$ increase and various events in the Southern Ocean (including reduced dust deposition and biological pump efficiency in the sub-Antarctic, a breakdown of polar Antarctic stratification, and sea ice retreat) has suggested to many that Southern Ocean processes are critical to carbon release from the deep ocean during glacial terminations. The deep

ocean $[CO_3^{2-}]$ history also highlights the importance of changes in the whole ocean alkalinity inventory (associated with carbonate compensation and coral reef buildup) on carbon reorganization in the ocean-atmosphere-land biosphere system. Existing deep ocean $[CO_3^{2-}]$ reconstructions are short and limited to a few locations. Development of high-resolution records since the last glacial and of reconstructions that span several glacial-interglacial cycles will improve and quantify our understanding of the role of deep ocean carbonate chemistry in past atmospheric CO_2 changes.

REFERENCES

Anderson, D.M., and D. Archer. 2002. Glacial-interglacial stability of ocean pH inferred from foraminifer dissolution rates. *Nature* 416:70–73, http://dx.doi.org/10.1038/416070a.

Anderson, R.F., S. Ali, L. Bradtmiller, S.H.H. Nielsen, M.Q. Fleisher, B.E. Anderson, and L.H. Burckle. 2009. Wind-driven upwelling in the Southern Ocean and the deglacial rise in atmospheric CO_2. *Science* 323:1,443–1,448, http://dx.doi.org/10.1126/science.1167441.

Anderson, R.F., M.Q. Fleisher, Y. Lao, and G. Winckler. 2008. Modern $CaCO_3$ preservation in equatorial Pacific sediments in the context of late-Pleistocene glacial cycles. *Marine Chemistry* 111:30–46, http://dx.doi.org/10.1016/j.marchem.2007.11.011.

Archer, D., and E. Maier-Reimer. 1994. Effect of deep-sea sedimentary calcite preservation on atmospheric CO_2 concentration. *Nature* 367:260–263, http://dx.doi.org/10.1038/367260a0.

Barker, S., and H. Elderfield. 2002. Foraminiferal calcification response to glacial-interglacial changes in atmospheric CO_2. *Science* 297:833–836, http://dx.doi.org/10.1126/science.1072815.

Berger, W.H. 1977. Deep-sea carbonate and deglaciation preservation spike in pteropods and foraminifera. *Nature* 269:301–304, http://dx.doi.org/10.1038/269301a0.

Bird, M.I., J. Lloyd, and G.D. Farquhar. 1994. Terrestrial carbon storage at the LGM. *Nature* 371:566, http://dx.doi.org/10.1038/371566a0.

Boyle, E.A. 1988. Vertical oceanic nutrient fractionation and glacial/interglacial CO_2 cycles. *Nature* 331:55–56, http://dx.doi.org/10.1038/331055a0.

Boyle, E.A., and L. Keigwin. 1987. North Atlantic thermohaline circulation during the past 20,000 years linked to high-latitude surface temperature. *Nature* 330:35–40, http://dx.doi.org/10.1038/330035a0.

Bradtmiller, L., R.F. Anderson, J. Sachs, and M.Q. Fleisher. 2010. A deeper respired carbon pool in the glacial equatorial Pacific Ocean. *Earth and Planetary Science Letters* 299:417–425, http://dx.doi.org/10.1016/j.epsl.2010.09.022.

Broecker, W. 1982. Glacial to interglacial changes in ocean chemistry. *Progress in Oceanography* 2:151–197, http://dx.doi.org/10.1016/0079-6611(82)90007-6.

Broecker, W., and S. Barker. 2007. A 190‰ drop in atmosphere's $\Delta^{14}C$ during the "Mystery Interval" (17.5 to 14.5 kyr). *Earth and Planetary Science Letters* 256:90–99, http://dx.doi.org/10.1016/j.epsl.2007.01.015.

Broecker, W., S.L. Peacock, R. Weiss, E. Fahrbach, M. Schroeder, U. Mikolajewicz, C. Heinze, R.M. Key, T.H. Peng, and S.I. Rubin. 1998. How much deep water is formed in the Southern Ocean? *Journal of Geophysical Research* 103:15,833–15,843, http://dx.doi.org/10.1029/98JC00248.

Broecker, W., and T.H. Peng. 1982. *Tracers in the Sea*. Eldigio Press, 690 pp.

Broecker, W., and T. Takahashi. 1978. The relationship between lysocline depth and in situ carbonate ion concentration. *Deep Sea Research* 25:65–95.

Broecker, W.S., and G.M. Henderson. 1998. The sequence of events surrounding Termination II and their implications for the cause of glacial-interglacial CO_2 changes. *Paleoceanography* 13:352–364, http://dx.doi.org/10.1029/98pa00920.

Broecker, W.S., and T.H. Peng. 1987. The role of $CaCO_3$ compensation in the glacial to interglacial atmospheric CO_2 change. *Global Biogeochemical Cycles* 1:15–29, http://dx.doi.org/10.1029/GB001i001p00015.

Brovkin, V., A. Ganopolski, D. Archer, and S. Rahmstorf. 2007. Lowering of glacial atmospheric CO_2 in response to changes in oceanic circulation and marine biogeochemistry. *Paleoceanography* 22, PA4202, http://dx.doi.org/10.1029/2006pa001380.

Brown, R.E., L.D. Anderson, E. Thomas, and J.C. Zachos. 2011. A core-top calibration of B/Ca in the benthic foraminifers *Nuttallides umbonifera* and *Oridorsalis umbonatus*: A proxy for Cenozoic bottom water carbonate saturation. *Earth and Planetary Science Letters* 310:360–368, http://dx.doi.org/10.1016/j.epsl.2011.08.023.

Burke, A., and L.F. Robinson. 2012. The Southern Ocean's role in carbon exchange during the last deglaciation. *Science* 355:557–561, http://dx.doi.org/10.1126/science.1208163.

Catubig, N.R., D. Archer, R. Francois, P. DeMenocal, W.R. Howard, and E.-F. Yu. 1998. Global deep-sea burial rate of calcium carbonate during the last glacial maximum. *Paleoceanography* 13:298–310, http://dx.doi.org/10.1029/98PA00609.

Ciais, P., A. Tagliabue, M. Cuntz, L. Bopp, M. Scholze, G. Hoffmann, A. Lourantou, S.P. Harrison, I.C. Prentice, D.I. Kelley, and others. 2012. Large inert carbon pool in the terrestrial biosphere during the Last Glacial Maximum. *Nature Geoscience* 5:74–79, http://dx.doi.org/10.1038/Ngeo1324.

Crowley, T.J. 1983. Calcium-carbonate preservation patterns in the central North Atlantic during the last 150,000 years. *Marine Geology* 51:1–14, http://dx.doi.org/10.1016/0025-3227(83)90085-3.

Curry, W.B., and D. Oppo. 2005. Glacial water mass geometry and the distribution of $\delta^{13}C$ of ΣCO_2 in the western Atlantic Ocean. *Paleoceanography* 20, PA1017, http://dx.doi.org/10.1029/2004PA001021.

Farrell, J.W., and W.L. Prell. 1989. Climatic change and $CaCO_3$ preservation: An 800,000 year bathymetric reconstruction from the central equatorial Pacific Ocean. *Paleoceanography* 4:447–466, http://dx.doi.org/10.1029/PA004i004p00447.

Farrell, J.W., and W.L. Prell. 1991. Pacific $CaCO_3$ preservation and $\delta^{18}O$ since 4 Ma: Paleoceanic and paleoclimatic implications. *Paleoceanography* 6:485–498, http://dx.doi.org/10.1029/91PA00877.

Galbraith, E.D., S.L. Jaccard, T.F. Pedersen, D.M. Sigman, G.H. Haug, M. Cook, J.R. Southon, and R. Francois. 2007. Carbon dioxide release from the North Pacific abyss during the last deglaciation. *Nature* 449:890–893, http://dx.doi.org/10.1038/nature06227.

Grant, K.M., E.J. Rohling, M. Bar-Matthews, A. Ayalon, M. Medina-Elizalde, C. Bronk Ramsey, C. Satow, and A.P. Roberts. 2012. Rapid coupling between ice volume and polar temperature over the past 150,000 years. *Nature* 491:744–747, http://dx.doi.org/10.1038/nature11593.

Hemming, N.G., and G.N. Hanson. 1992. Boron isotopic composition and concentration in modern marine carbonates. *Geochimica et Cosmochimica Acta* 56:537–543, http://dx.doi.org/10.1016/0016-7037(92)90151-8.

Henehan, M.J., J. Rae, G.L. Foster, J. Erez, K.C. Prentice, M. Kucera, H.C. Bostock, M.A. Martinez-Boti, J.A. Milton, P.A. Wilson, and others. 2013. Calibration of the boron isotope proxy in the planktonic foraminifera *Globigerinoides ruber* for use in palaeo-CO_2

reconstruction. *Earth and Planetary Science Letters* 364:111–122, http://dx.doi.org/10.1016/j.epsl.2012.12.029.

Hodell, D.A., C.D. Charles, and F.J. Sierro. 2001. Late Pleistocene evolution of the ocean's carbonate system. *Earth and Planetary Science Letters* 192:109–124, http://dx.doi.org/10.1016/S0012-821X(01)00430-7.

Hönisch, B., T. Bickert, and N.G. Hemming. 2008. Modern and Pleistocene boron isotope composition of the benthic foraminifer *Cibicidoides wuellerstorfi*. *Earth and Planetary Science Letters* 272:309–318, http://dx.doi.org/10.1016/j.epsl.2008.04.047.

Jaccard, S.L., and E.D. Galbraith. 2012. Large climate-driven changes of oceanic oxygen concentrations during the last deglaciation. *Nature Geoscience* 5:151–156, http://dx.doi.org/10.1038/Ngeo1352.

Jouzel, J., V. Masson-Delmotte, O. Cattani, G. Dreyfus, S. Falourd, G. Hoffmann, B. Minster, J. Nouet, J.M. Barnola, J. Chappellaz, and others. 2007. Orbital and millennial Antarctic climate variability over the past 800,000 years. *Science* 317:793–797, http://dx.doi.org/10.1126/science.1141038.

Key, R.M., A. Kozyr, C.L. Sabine, K. Lee, R. Wanninkhof, J.L. Bullister, R.A. Feely, F.J. Millero, C. Mordy, and T.H. Peng. 2004. A global ocean carbon climatology: Results from Global Data Analysis Project (GLODAP). *Global Biogeochemical Cycles* 18, GB4031, http://dx.doi.org/10.1029/2004GB002247.

Kumar, N., R.F. Anderson, R.A. Mortlock, P.N. Froelich, P. Kubik, B. Dittrichhannen, and M. Suter. 1995. Increased biological productivity and export production in the glacial Southern Ocean. *Nature* 378:675–680, http://dx.doi.org/10.1038/378675a0.

Le, J., and N.J. Shackleton. 1992. Carbonate dissolution fluctuations in the Western equatorial Pacific during the late Quaternary. *Paleoceanography* 7:21–42, http://dx.doi.org/10.1029/91PA02854.

Lemarchand, D., J. Gaillardet, E. Lewin, and C.J. Allegre. 2000. The influence of rivers on marine boron isotopes and implications for reconstructing past ocean pH. *Nature* 408:951–954, http://dx.doi.org/10.1038/35050058.

Lisiecki, L.E., and M.E. Raymo. 2005. A Pliocene-Pleistocene stack of 57 globally distributed benthic δ^{18}O records. *Paleoceanography* 20, PA1003, http://dx.doi.org/10.1029/2004PA001071.

Lund, D.C., J.F. Adkins, and R. Ferrari. 2011. Abyssal Atlantic circulation during the Last Glacial Maximum: Constraining the ratio between transport and vertical mixing. *Paleoceanography* 26, PA1213, http://dx.doi.org/10.1029/2010pa001938.

Lüthi, D., M.L. Floch, B. Bereiter, T. Blunier, J.M. Barnola, U. Siegenthaler, D. Raynaud, J. Jouzel, H. Fischer, K. Kawamura, and T.F. Stocker. High-resolution carbon dioxide concentration record 650,000–800,000 years before present. *Nature* 453:379–382, http://dx.doi.org/10.1038/nature06949.

Lutze, G.F., and H. Thiel. 1989. Epibenthic foraminifera from elevated microhabitats: *Cibicidoides wuellerstorfi* and *Planulina ariminensis*. *Journal of Foraminiferal Research* 19:153–158.

Marchitto, T.M., W.B. Curry, and D.W. Oppo. 2000. Zinc concentrations in benthic foraminifera reflect seawater chemistry. *Paleoceanography* 15:299–306, http://dx.doi.org/10.1029/1999PA000420.

Martinez-Garcia, A., A. Rosell-Mele, S.L. Jaccard, W. Geibert, D.M. Sigman, and G.H. Haug. 2011. Southern Ocean dust-climate coupling over the past four million years. *Nature* 476:312–315, http://dx.doi.org/10.1038/nature10310.

Menviel, L., and F. Joos. 2012. Toward explaining the Holocene carbon dioxide and carbon isotope records: Results from transient ocean carbon cycle-climate simulations. *Paleoceanography* 27, PA1207, http://dx.doi.org/10.1029/2011pa002224.

Opdyke, B.N., and J.C.G. Walker. 1992. Return of the coral reef hypothesis: Basin to shelf partitioning of $CaCO_3$ and its effect on atmospheric CO_2. *Geology* 20:733–736, http://dx.doi.org/10.1130/0091-7613(1992)020<0733:ROTCRH>2.3.CO;2.

Rae, J.W.B., G.L. Foster, D.N. Schmidt, and T. Elliott. 2011. Boron isotopes and B/Ca in benthic foraminifera: Proxies for the deep ocean carbonate system. *Earth and Planetary Science Letters* 302:403–413, http://dx.doi.org/10.1016/j.epsl.2010.12.034.

Raitzsch, M., E.C. Hathorne, H. Kuhnert, J. Groeneveld, and T. Bickert. 2011. Modern and late Pleistocene B/Ca ratios of the benthic foraminifer *Planulina wuellerstorfi* determined with laser ablation ICP-MS. *Geology* 39:1,039–1,042, http://dx.doi.org/10.1130/G32009.1.

Rickaby, R.E.M., H. Elderfield, N. Roberts, C.-D. Hillenbrand, and A. Mackensen. 2010. Evidence for elevated alkalinity in the glacial Southern Ocean. *Paleoceanography* 25, PA1209, http://dx.doi.org/10.1029/2009PA001762.

Ridgwell, A.J., A.J. Watson, M.A. Maslin, and J.O. Kaplan. 2003. Implications of coral reef buildup for the controls on atmospheric CO_2 since the Last Glacial Maximum. *Paleoceanography* 18, 1083, http://dx.doi.org/10.1029/2003PA000893.

Sanyal, A., N.G. Hemming, G.N. Hanson, and W.S. Broecker. 1995. Evidence for a higher pH in the glacial ocean from boron isotopes in foraminifera. *Nature* 373:234–236, http://dx.doi.org/10.1038/373234a0.

Schlitzer, R., 2006. Ocean Data View, http://odv.awi-bremerhaven.de.

Schmitz, W.J. 1996. *On the World Ocean Circulation,* vol. II. *The Pacific and Indian Ocean: A Global Update.* Technical Report WHOI-96-08, Woods Hole Oceanographic Institution, Woods Hole, MA.

Sigman, D.M., and E.A. Boyle. 2000. Glacial/interglacial variations in atmospheric carbon dioxide. *Nature* 407:859–869, http://dx.doi.org/10.1038/35038000.

Sigman, D.M., M.P. Hain, and G.H. Haug. 2010. The polar ocean and glacial cycles in atmospheric CO_2 concentration. *Nature* 466:47–55, http://dx.doi.org/10.1038/Nature09149.

Stephens, B.B., and R.F. Keeling. 2000. The influence of Antarctic sea ice on glacial-interglacial CO_2 variations. *Nature* 404:171–174, http://dx.doi.org/10.1038/35004556.

Toggweiler, J.R., J.L. Russell, and S.R. Carson. 2006. Midlatitude westerlies, atmospheric CO_2, and climate change during the ice ages. *Paleoceanography* 21, PA2005, http://dx.doi.org/10.1029/2005PA001154.

Yu, J., R.F. Anderson, Z.D. Jin, J. Rae, B.N. Opdyke, and S. Eggins. 2013a. Responses of the deep ocean carbonate system to carbon reorganization during the Last Glacial–interglacial cycle. *Quaternary Science Reviews* 76:39–52, http://dx.doi.org/10.1016/j.quascirev.2013.06.020.

Yu, J., W. Broecker, H. Elderfield, Z.D. Jin, J. McManus, and F. Zhang. 2010a. Loss of carbon from the deep sea since the Last Glacial Maximum. *Science* 330:1,084–1,087, http://dx.doi.org/10.1126/science.1193221.

Yu, J.M., and H. Elderfield. 2007. Benthic foraminiferal B/Ca ratios reflect deep water carbonate saturation state. *Earth and Planetary Science Letters* 258:73–86, http://dx.doi.org/10.1016/j.epsl.2007.03.025.

Yu, J.M., H. Elderfield, and A. Piotrowski. 2008. Seawater carbonate ion-δ^{13}C systematics and application to glacial-interglacial North Atlantic ocean circulation. *Earth and Planetary Science Letters* 271:209–220, http://dx.doi.org/10.1016/j.epsl.2008.04.010.

Yu, J., G.L. Foster, H. Elderfield, W.S. Broecker, and E. Clark. 2010b. An evaluation of benthic foraminiferal B/Ca and δ^{11}B for deep ocean carbonate ion and pH reconstructions. *Earth and Planetary Science Letters* 293:114–120, http://dx.doi.org/10.1016/j.epsl.2010.02.029.

Yu, J., D.J.R. Thornalley, J. Rae, and I.N. McCave. 2013b. Calibration and application of B/Ca, Cd/Ca, and δ^{11}B in *Neogloboquadrina pachyderma* (sinistral) to constrain CO_2 uptake in the subpolar North Atlantic during the last deglaciation. *Paleoceanography* 28:237–252, http://dx.doi.org/10.1002/palo.20024.

Zeebe, R.E., and D.A. Wolf-Gladrow. 2001. *CO_2 in Seawater: Equilibrium, Kinetics, Isotopes.* Elsevier, Amsterdam, 360 pp.